Supporting Information

Revealing the compositional effect on the intrinsic long-term stability of perovskite solar cells

Liqiang Xie, Peiquan Song, Lina Shen, Jianxun Lu, Kaikai Liu, Kebin Lin, Wenjing Feng, Chengbo Tian, Zhanhua Wei*

Institute of Luminescent Materials and Information Displays, College of Materials Science & Engineering, Huaqiao University, Xiamen, 361021, China.

E-mail: weizhanhua@hqu.edu.cn

1. Experimental

1.1 Materials

Unless otherwise stated, all chemical reagents and materials were purchased from Sigma-Aldrich and used as received.

1.2 Devices fabrication

Pre-patterned fluorine-doped tin oxide-coated glasses (NSG TEC A7) were firstly washed using a cleanser, and then sequentially treated by ultrasonication in deionized water, acetone, isopropanol, and ethanol for 20 min, respectively. A ~30 nm of compact TiO_2 blocking layer was deposited onto the UV-Ozone treated FTO by spray-pyrolysis, which was carried out at 450 ^oC using a precursor solution of titanium diisopropoxide bis(acetylacetonate) diluted with ethanol and a carrier gas of O_2. After spraying, the samples were annealed at 450 ^oC for another 20 min to improve their electronic properties. To deposit the TiO_2 mesoporous layer, TiO_2 paste (Great Solar, 30 NRD) was firstly diluted in ethanol with a weight ratio of 1 : 6, then spin-coated onto the as-prepared TiO_2 compact layer at a speed of 5,000 rpm for 20 s with a ramp-up of 2,000 rpm s^{-1}. The resultant films were heated at 100 ^oC for 10 min to remove the solvents and then sintered at 500 ^oC for 30 min. After cooling down to 150 ^oC, the substrates were immediately transferred into a N_2-filled glovebox. The pristine CsFA precursor was prepared by mixing 1.1 mmol of PbI_2, 1 mmol of FAI, 45 μL of CsI solution (1.5 M in DMSO) in a mixed solvent of DMF (608 μL) and DMSO (152 μL). Then the precursor solution of CsFA–Br and CsFA–Br–MA were obtained by adding 0.01 mmol of $CsPbBr_3$ and 0.01 mmol of ($PbBr_2$ + MABr) into the pristine CsFA precursor,

respectively. 40 μL of the perovskite precursor solution was spread on the substrate and spin-coated in a two-step procedure at 1,000 rpm and 5,000 rpm for 10 s and 20 s, respectively. During the second step, 180 μL of chlorobenzene was dripped on the spinning substrate at the 25th second of the procedure. The as-deposited perovskite intermediate film was immediately annealed on a hotplate at 100 ^{o}C for 60 min. A glass petri dish was used to cover the annealing samples in the first 2 min during the annealing process. After cooling down to room temperature, a 200 nm thick bis(trifluoromethane)sulfonimide lithium salt and tert-butylpyridine doped Spiro-OMeTAD layer was coated onto the perovskite film as hole transporting layer. Finally, a 60 nm of gold back contact electrode was deposited by thermal evaporation to finish the fabrication of the whole device.

1.3 Solar cell characterization

The perovskite solar cells (PSCs) devices were stored in a dark electronic drying cabinet with relative humidity below 10%. *J–V* curves were measured using Keithley 2400 in a N_2-filled glovebox, and under simulated AM 1.5G conditions (Enli tech, AAA solar simulator). The light intensity was calibrated using an NREL-calibrated Si solar cell with KG-5 filter. To guarantee the accuracy of *J–V* curves measurements, a metal mask was placed in front of the solar cell to determine the exact active area (0.12 cm^2). Incident photon-to-electron conversion efficiency (IPCE) was measured on an IPCE system (Enli tech, QE-R666) and the integrated current density at the short circuit was compared with that extracted from *J–V* scans. Long–term operational stability of PSCs was tested using a measurement kit developed by Suzhou D&R Instruments Co., Ltd.,

in which a LED lamp with intensity of 100 mW cm^{-2} was used as light source, and a source meter with multi channels was controlled by a software to run maximum power point (MPP) tracking and *J–V* tests.

1.4 Additional materials characterization

UV-vis absorption spectroscopy for Tauc plot analysis and photoluminescence spectroscopy were acquired in a N_2-filled glovebox with a flame spectrometer (Ocean Optics). XRD measurements were carried out on a D8 Advance diffractometer (Bruker AXS) with Cu Kα radiation source. SEM was performed using a field-emission scanning electron microscope (Hitachi S-8000). Space-charge-limited current (SCLC) was performed by measuring the dark *I–V* curves of the simplified devices of FTO/perovskite/Au on a CHI660E potentiostat. Electrochemical impedance spectroscopy (EIS) was also performed on CHI660E. The light intensity dependence tests were measured under light illumination of the solar simulator in a N_2-filled glovebox.

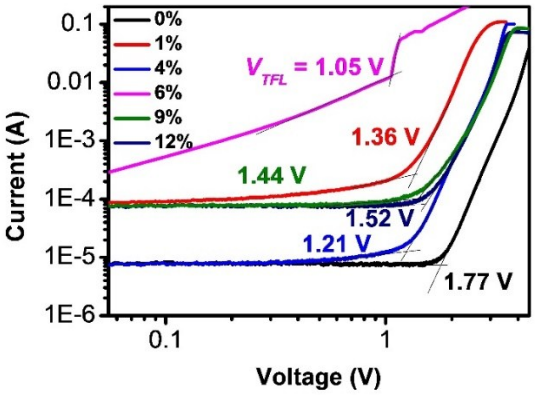

Fig. S1 Space-charge-limited current (SCLC) measurements of perovskite films with Br ratio of 0%, 1%, 4%, 6%, 9%, and 12%.

Table S1 Trap state density of perovskite films with different Br ratio. Note that the doping content of Cs is also varied because the used dopant is $CsPbBr_3$ to keep the stoichiometry of perovskite. The V_{TFL} value of perovskite film with 6% Br is determined according to our previously reported work (reference 32).

Br ratio	0%	1%	4%	6%	9%	12%
V_{TFL} (V)	1.77	1.36	1.21	1.05	1.44	1.52
n_{trap} (10^{16} cm^{-1})	2.74	2.11	1.87	1.63	2.24	2.36

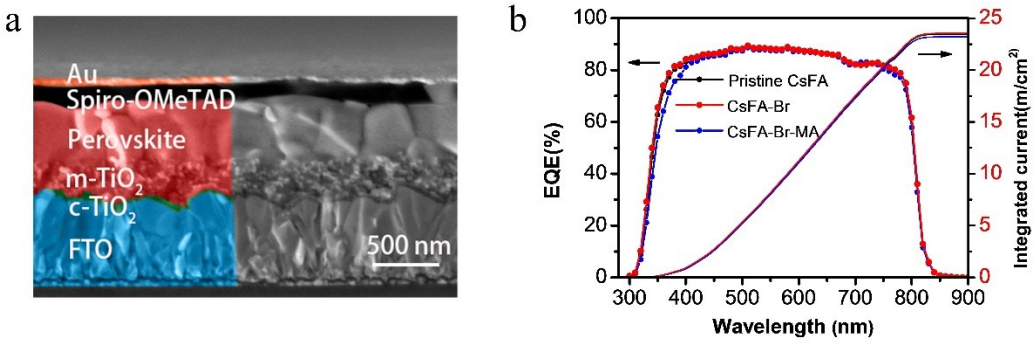

Fig. S2 (a) Cross-sectional SEM image of a typical PSC, showing a device configuration of FTO/c-TiO_2/m-TiO_2/Perovskite/Spiro-OMeTAD/Au. (b) IPCE spectra of PSCs with different perovskite composition. The integrated J_{SC} for pristine CsFA, CsFA–Br, and CsFA–Br–MA is 23.46, 23.56, and 23.22 mA cm^{-2}, respectively.

Table S2 *J–V* parameters of the freshly fabricated PSCs with perovskite composition of pristine CsFA, CsFA–Br, and CsFA–Br–MA.

Perovskite	J_{SC} / mA cm^{-2}	V_{OC}/V	FF	PCE/%
Pristine CsFA	24.65	0.998	0.532	13.08
CsFA–Br	24.40	1.043	0.707	18.00
CsFA–Br–MA	24.39	1.004	0.558	13.67

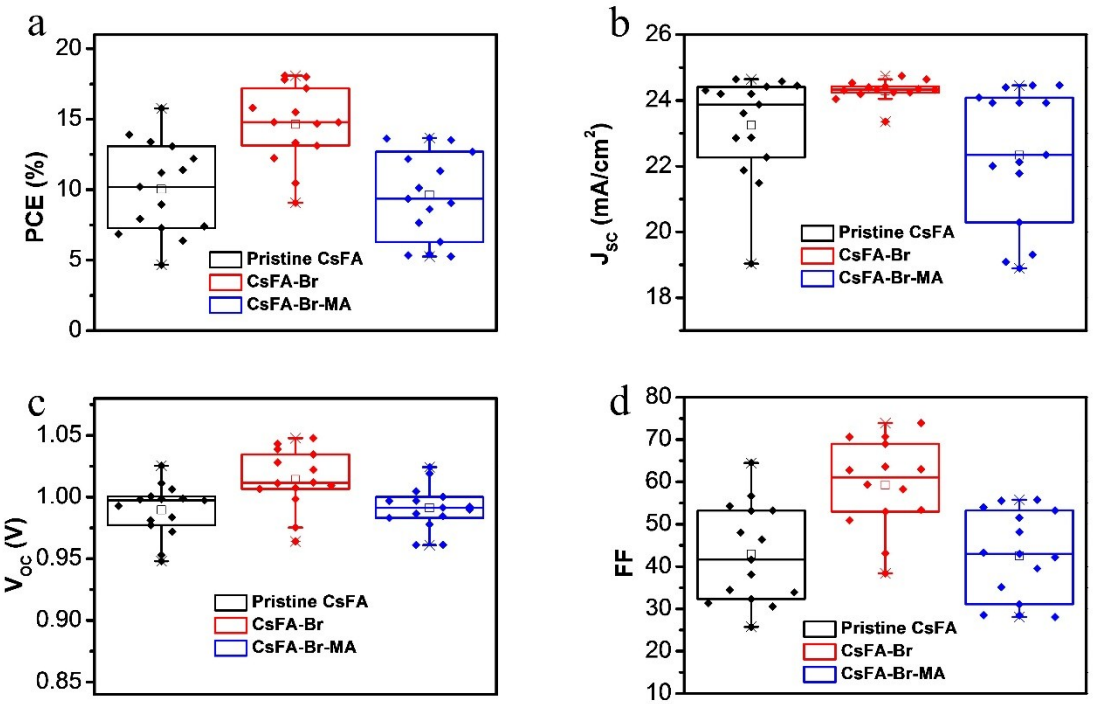

Fig. S3 Statistical results of (a) PCE, (b) J_{SC}, (c) V_{OC}, and (d) FF from one batch of 14 freshly fabricated PSCs.

Table S3 *J–V* parameters of the PSCs after light soaking with perovskite composition of pristine CsFA, CsFA–Br, and CsFA–Br–MA.

Perovskite	J_{SC} / mA cm^{-2}	V_{OC} / V	FF	PCE/%
Pristine CsFA	25.02	1.052	0.765	20.16
CsFA–Br	24.91	1.053	0.776	20.36
CsFA–Br–MA	24.94	1.052	0.771	20.22

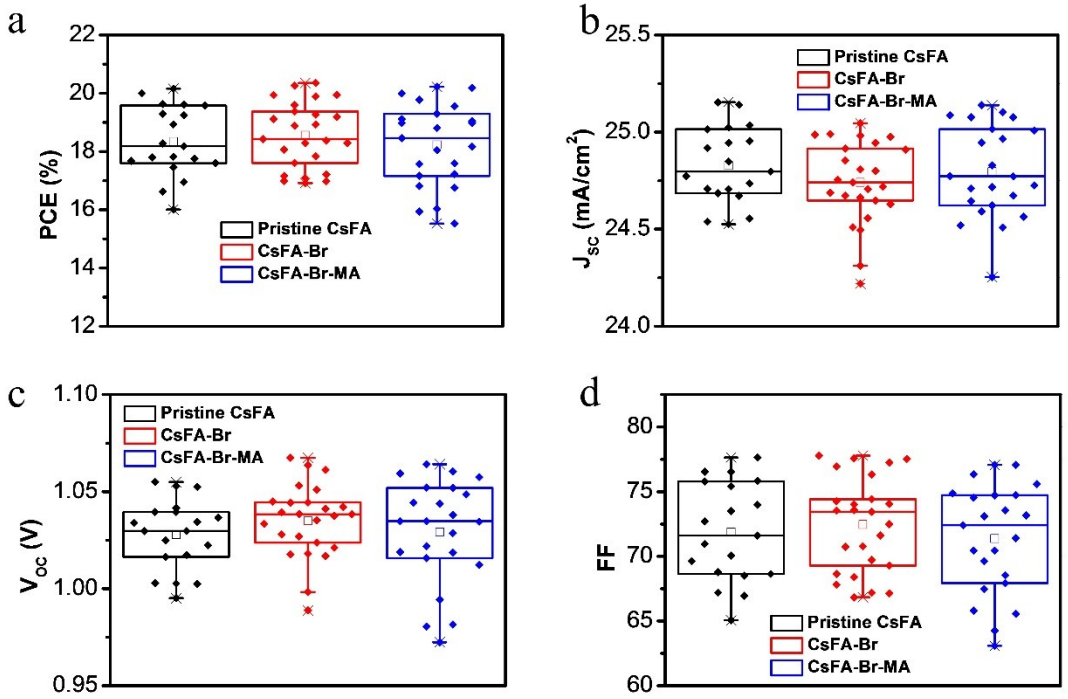

Fig. S4 Statistical results of (a) PCE, (b) J_{SC}, (c) V_{OC}, and (d) FF from one batch of 19 PSCs of pristine CsFA, 25 PSCs of CsFA–Br, and 23 PSCs of CsFA–Br–MA after light soaking.

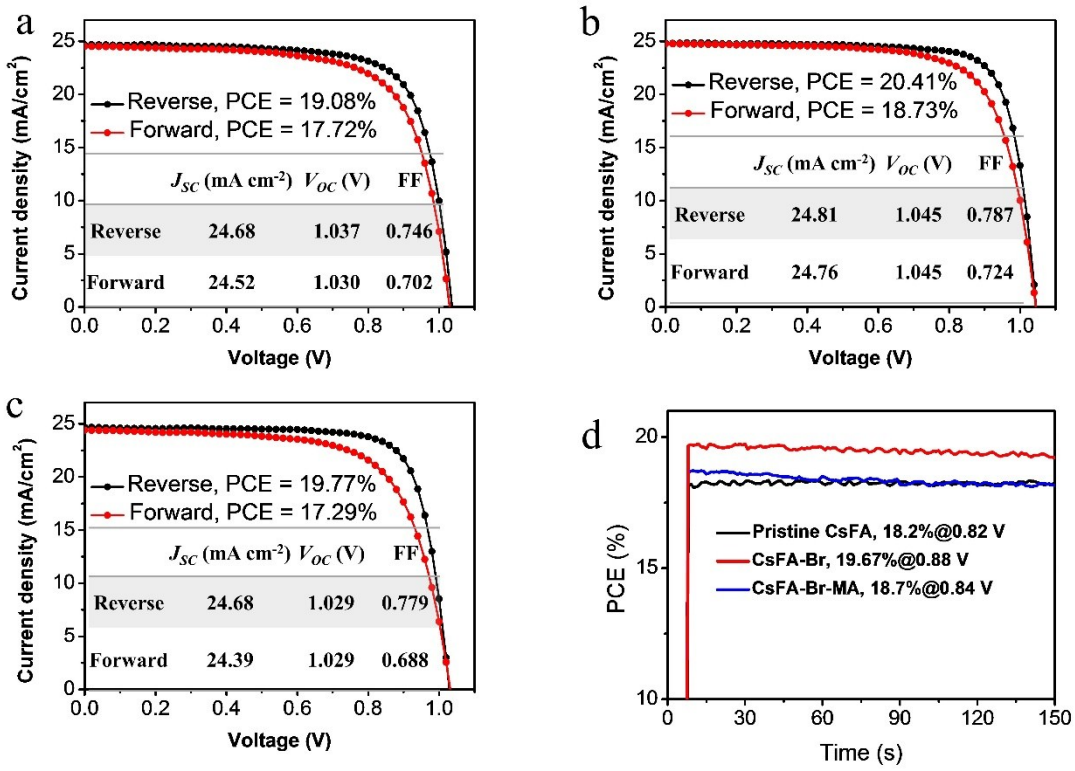

Fig. S5 Hysteresis of PSCs with different perovskite composition. *J-V* curves of PSCs measured by both reverse (from 1.2 to -0.2 V) and forward scan direction of the devices: (a) Pristine CsFA, (b) CsFA–Br, and (c) CsFA–Br–MA. (d) Steady-state output of PSCs for pristine CsFA, CsFA–Br, and CsFA–Br–MA.

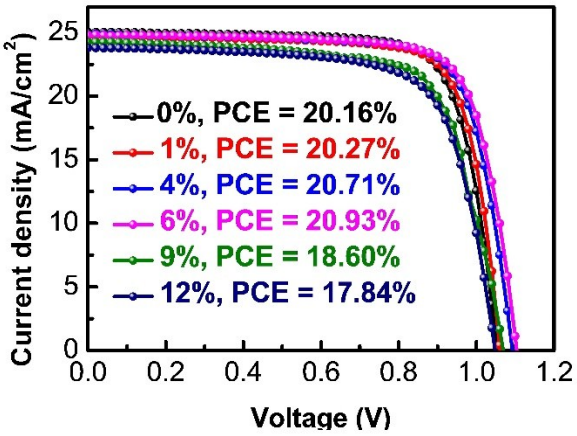

Fig. S6 *J–V* curves of PSCs fabricated with different doping content of Br. Note that the doping content of Cs is also varied because the used dopant is $CsPbBr_3$ to keep the stoichiometry of perovskite.

Table S4 *J–V* parameters of the PSCs fabricated with different doping content of Br. Note that the doping content of Cs is also varied because the used dopant is $CsPbBr_3$ to keep the stoichiometry of perovskite.

	J_{SC} / mA cm^2	V_{OC} / V	FF	PCE /%
0%	**25.02**	**1.052**	**0.765**	**20.16**
1%	**24.72**	**1.061**	**0.772**	**20.27**
4%	**24.83**	**1.092**	**0.763**	**20.71**
6%	**24.82**	**1.104**	**0.764**	**20.93**
9%	**24.33**	**1.069**	**0.715**	**18.60**
12%	**23.79**	**1.048**	**0.714**	**17.84**

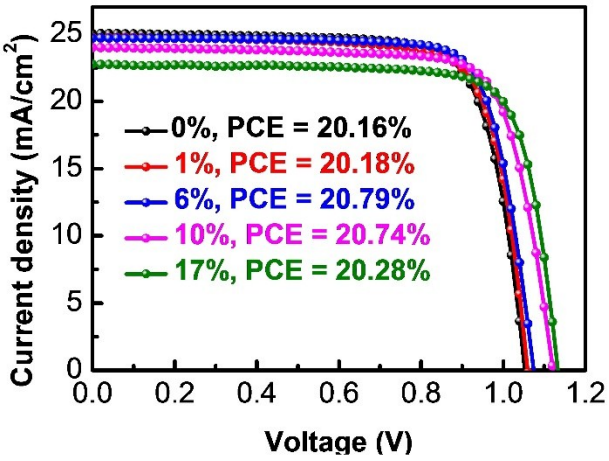

Fig. S7 *J–V* curves of PSCs fabricated with different doping content of MA and Br. The used dopant is $MAPbBr_3$ to keep the stoichiometry of perovskite.

Table S5 *J–V* parameters of the PSCs fabricated with different doping content of MA and Br. The used dopant is $MAPbBr_3$ to keep the stoichiometry of perovskite.

	J_{SC} / mA cm^2	V_{OC} / V	FF	PCE /%
0%	**25.02**	**1.052**	**0.765**	**20.16**
1%	**24.72**	**1.059**	**0.771**	**20.18**
6%	**24.68**	**1.074**	**0.784**	**20.79**
10%	**23.98**	**1.121**	**0.771**	**20.74**
17%	**22.74**	**1.133**	**0.787**	**20.28**

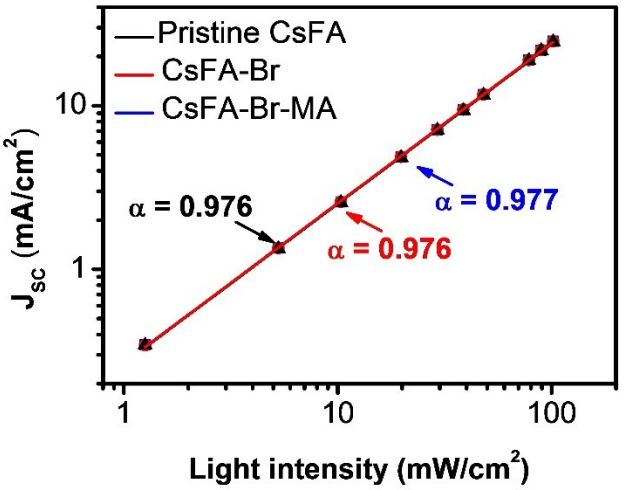

Fig. S8 Light intensity dependence of J_{SC} for pristine CsFA, CsFA–Br, and CsFA–Br–MA PSCs.

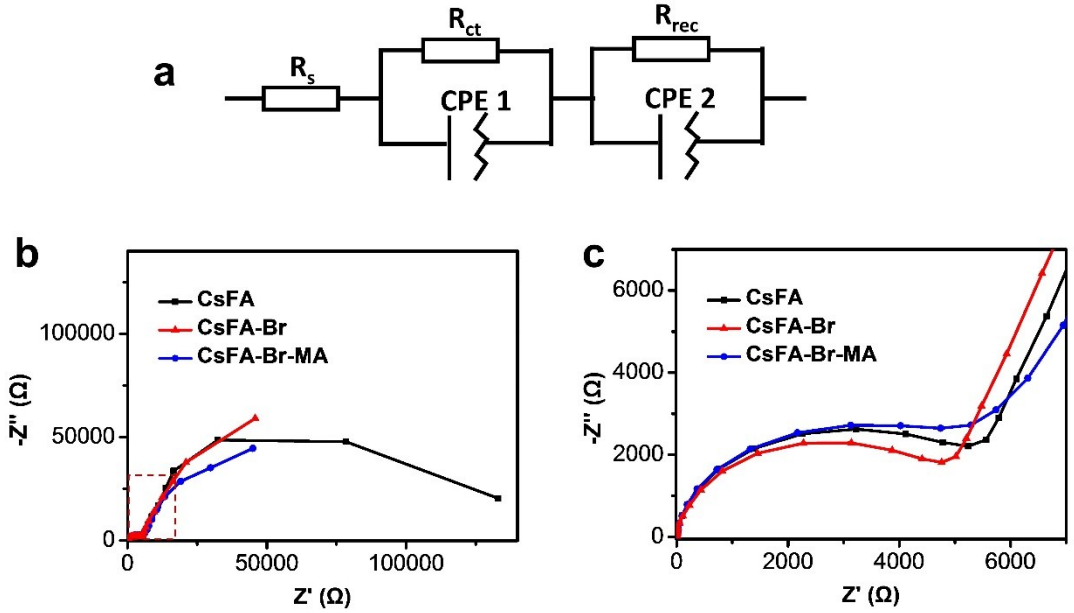

Fig. S9 Electrochemical impedance spectroscopy (EIS) study of PSCs of CsFA, CsFA–Br and CsFA–Br–MA. (a) Equivalent circuit of PSCs. (b) EIS spectra of PSCs measured at short circuit and under 0.01 sun illumination. (c) Insect of the high-frequency region of b.